Dehydrogenation vs Oxygenation in Photosensitized Oxidation of 9-Substituted 10-Methyl-9,10-dihydroacridine in the Presence of Scandium Ion

Shunichi Fukuzumi,*,† Shunsuke Fujita,† Tomoyoshi Suenobu,† Hiroshi Imahori,† Yasuyuki Araki,‡ and Osamu Ito*,‡

Department of Material and Life Science, Graduate School of Engineering, Osaka University, CREST, Japan Science and Technology Corporation (JST), Suita, Osaka 565-0871, Japan, and Institute of Multidisciplinary Research for Advanced Materials, Tohoku University, CREST, Japan Science and Technology Corporation (JST), Sendai, Miyagi 980-8577, Japan

Received: July 25, 2001; In Final Form: November 5, 2001

Photooxidation of 9-substituted 10-methyl-9,10-dihydroacridine (AcrHR) with oxygen occurs efficiently in the presence of 9,10-dicyanoanthracene (DCA) and scandium triflate [$Sc(OTf)_3$] under visible light irradiation in oxygen-saturated acetonitrile (MeCN) to yield the 9-substituted 10-methylacridinium ion ($AcrR^+$) and H_2O_2 or the 10-methylacridinium ion ($AcrH^+$) and the oxygenated products of R such as ROOH, depending on the type of substitutent R. No DCA-photosensitized oxidation of AcrHR occurs in the absence of Sc^{3+} under otherwise the same experimental conditions. The observed selectivities for the C(9)−H vs C(9)−C bond cleavage of AcrHR in the DCA-photosensitized oxidation of AcrHR in the presence of $Sc(OTf)_3$ agree with those for the cleavage of radical cations of AcrHR ($AcrHR^{\bullet+}$) depending on the type of substituent R. Such product selectivities, being consistent with the electron-transfer oxidation of AcrHR, combined with quantum yield determination, the $^1O_2$ phosphorescence decay dynamics, and the detection of radical ion intermediates in the laser-flash photolysis experiments reveal the electron-transfer radical chain mechanism for the DCA-photosensitized oxidation of AcrHR initiated by photoinduced electron transfer from AcrHR to the singlet excited state of DCA.

Introduction

Reduced nicotinamide adenine dinucleotide (NADH) plays a vital role as the electron source in the respiratory chain to reduce oxygen to water.[1] NADH itself is stable to oxygen, and thus, either oxygen or NADH should be activated to undergo the reduction of oxygen by NADH.[2,3] In the former case, activated oxygen species such as singlet oxygen have been reported to oxidize NADH to yield the two-electron oxidized form, i.e., NAD^+.[4,5] In the latter case, photoinduced electron transfer from the singlet excited state of NADH and analogues to oxygen initiates the reduction of oxygen in the protic media to hydrogen peroxide.[6,7]

Singlet oxygen is normally produced by photosensitization,[8] and a variety of substrates are oxygenated by the reactions with singlet oxygen.[9−12] Cyanoaromatic compounds such as 9,10-dicyanoanthracene (DCA) have frequently been used as sensitizers for the formation of singlet oxygen.[13−16] However, a sensitizer for the formation of singlet oxygen is often converted to the radical ion by the photoinduced electron-transfer reactions in the presence of an electron donor or acceptor.[17−19] Both $O_2^{\bullet-}$ and $^1O_2$ can be formed under the same reaction conditions, resulting in a competition between two different types of oxidation reactions.[15−17] To further complicate matters, $^1O_2$ can be reduced to $O_2^{\bullet-}$ by thermal and photoinduced electron transfer from electron donors.[16] Thus, considerable care must be taken in assigning the mechanisms of photosensitized oxidation reactions with oxygen. Both transient dynamics of the intermediate radical ions and the careful product analysis are required to disclose the operating reaction mechanism. No such study has ever been performed for photosensitized oxidation of NADH analogues with oxygen.

We have previously found that the electron-transfer oxidation of 9-substituted 10-methyl-9,10-dihydroacridine (AcrHR), which is an acid stable NADH analogue, results in cleavage of the C(9)−H or C(9)−C bond depending on the type of the substituent R to yield the 9-substituted 10-methylacridinium ion ($AcrR^+$) or 10-methylacridinium ion ($AcrH^+$).[20] We report herein that the DCA-photosensitized oxidation of AcrHR by O_2 occurs efficiently in the presence of scandium triflate [$Sc(OTf)_3$] leading to the cleavage of the C(9)−H or C(9)−C bond of AcrHR to yield $AcrR^+$ and H_2O_2 (dehydrogenation) or $AcrH^+$ and the oxygenated products of R such as ROOH (oxygenation). The scandium ion (Sc^{3+}) is chosen as an effective promoter for the reduction of O_2, because Sc^{3+} has been reported to be the most effective catalyst among a variety of metal ions in the electron-transfer reduction of O_2.[21,22] The ratio of dehydrogenation vs oxygenation varies depending on the type of R. No photosensitized oxidation of AcrHR was observed in the absence of Sc^{3+} under otherwise the same experimental conditions. The possible role of $^1O_2$ and the detailed mechanism of the Sc^{3+}-promoted photosensitized oxidation of AcrHR by O_2 (dehydrogenation vs oxygenation) are carefully examined for the first time based on the product analysis, quantum yield determination, and the detection of radical ion intermediates in the laser-flash photolysis experiments.

* To whom correspondence should be addressed. E-mail: fukuzumi@ap.chem.eng.osaka-u.ac.jp.
† Osaka University.
‡ Tohoku University.

10.1021/jp0128729 CCC: $22.00
Published on Web 01/29/2002

Experimental Section

Materials. AcrHR was prepared from 10-methylacridinium iodide ($AcrH^+I^-$) by reduction with $NaBH_4$ in methanol and purified by recrystallization from ethanol.[23] $AcrH^+I^-$ was prepared by the reaction of acridine with methyl iodide in acetone and was converted to the perchlorate salt ($AcrH^+ClO_4^-$) by the addition of magnesium perchlorate to the iodide salt ($AcrH^+I^-$) and purified by recrystallization from methanol.[24] [9,9′-$^2H_2$]-10-Methyl-9,10-dihydroacridine ($AcrD_2$) was prepared from 10-methylacridone by reduction with $LiAlD_4$, which was obtained from Aldrich. 9-Alkyl (or phenyl)-10-methyl-9,10-dihydroacridines (AcrHR; R = Me, Et, CH_2Ph, Bu^t and Ph) were prepared by the reduction of $AcrH^+I^-$ with the corresponding Grignard reagents (RMgX).[20] 10,10′-Dimethyl-9,9′,-10,10′-tetrahydro-9,9′-biacridine [$(AcrH)_2$] was prepared from the reduction of 10-methylacridinium perchlorate ($AcrH^+ClO_4^-$) with $Me_3SnSnMe_3$ in MeCN at 333 K[25] and purified by recrystallization from the mixture of acetonitrile (MeCN) and chloroform. Anal. Calcd for $C_{28}H_{24}N_2$: C, 86.56; H, 6.23; N, 7.21. Found: C, 86.56; H, 6.29; N, 7.15. 9,10-Dicyanoanthracene (DCA) was obtained from Tokyo Kasei Organic Chemicals. Scandium trifluoromethanesulfonate, $Sc(OTf)_3$ (99%, F.W. = 492.16) was obtained from Pacific Metals Co., Ltd. (Taiheiyo Kinzoku). 7-Amino-4-methylcoumarin (coumarin 120) for the laser dye was purchased from Lambda Physik. *tert*-Butyl alcohol and benzaldehyde were obtained from Wako Pure Chemicals. Bu^{t}OOH was obtained from Nacalai Tesque Co., Ltd. Potassium ferrioxalate used as an actinometer was prepared according to the literature and purified by recrystallization from hot water.[26] MeCN and propionitrile (EtCN) as solvents were purified and dried by the standard procedure.[27] Deuterated [$^2H_3$]acetonitrile (CD_3CN, 99.8%) was obtained from EURI SOTOP, CEA, France and used as received.

Reaction Procedure. Typically, AcrHR (6.0×10^{-3} M), DCA (3.0×10^{-4} M), $Sc(OTf)_3$ (3.0×10^{-4} M), and CF_3COOH (1.0×10^{-2} M) were added to an NMR tube which contained an O_2-saturated CD_3CN solution (0.60 cm^3). The solution was irradiated for 1 h with a Xe lamp ($\lambda > 380$ nm) equipped with a Toshiba UV-37 cut off filter. The oxidized products of AcrHR were identified by the ^1H NMR spectra by comparing with those of authentic samples. The ^1H NMR measurements were performed using a JEOL JNM-AL-300 (300 MHz) NMR spectrometer. ^1H NMR (CD_3CN): $AcrH^+ClO_4^-$: δ 4.76 (s, 3H), 7.9−8.8 (m, 8H), 9.87 (s, 1H); $AcrMe^+ClO_4^-$: δ 3.48 (s, 3H), 4.74 (s, 3H), 7.9−8.9 (m, 8H); $AcrEt^+ClO_4^-$: δ 1.52 (t, 3H, J = 7.5 Hz), 3.95 (q, 2H, J = 7.5 Hz), 4.71 (s, 3H), 7.9−8.9 (m, 8H); $AcrPh^+ClO_4^-$: δ 4.83 (s, 3H), 7.5−8.6 (m, 13H); $AcrCH_2Ph^+ClO_4^-$: δ 4.79 (s, 3H), 5.35 (s, 2H), 7.5−8.9 (m, 13H); Bu^{t}OOH: δ 1.18 (s, 9H); Bu^{t}OH: δ 1.17 (s, 9H); PhCHO: δ 10.00 (s, 1H), 7.5−8.0 (m, 5H); $PhCH_2OOH$: δ 4.89 (s, 2H), 7.5−8.0 (m, 5H). The amounts of H_2O_2 formed in the photooxidation of AcrHR were determined by the titration with iodide ion according to the procedure as described previously.[28]

Quantum Yield Determination. A standard actinometer (potassium ferrioxalate)[26] was used for the quantum yield determination of the photooxidation of AcrHR in the presence of $Sc(OTf)_3$ and DCA in O_2-saturated MeCN. A 10 mm square quartz cuvette which contained an O_2-saturated MeCN solution (3.0 cm^3) of AcrHR, DCA (1.0×10^{-4} M), and $Sc(OTf)_3$ was irradiated with monochromatized light of $\lambda = 422$ nm using a Shimadzu spectrofluorophotometer (RF-5000). Under the condition of actinometry experiments, the actinometer absorbed essentially all the incident light of $\lambda = 422$ nm and DCA absorbed 95% of incident light of $\lambda = 422$ nm. The light intensity of monochromatized light of $\lambda = 422$ nm was determined as 1.6×10^{-9}, 2.5×10^{-9}, and 8.8×10^{-9} einstein s^{-1} with the slit width of 10, 15, and 20 nm, respectively. The photochemical reactions were monitored using a Hewlett Packard 8453 diode array spectrophotometer. The quantum yields were determined from the increase in absorbance due to $AcrH^+$ ($\lambda_{max} = 358$ nm, $\epsilon_{max} = 1.8 \times 10^4$ M^{-1} cm^{-1}), $AcrMe^+$ ($\lambda_{max} = 358$ nm, $\epsilon_{max} = 1.8 \times 10^4$ M^{-1} cm^{-1}), $AcrEt^+$ ($\lambda_{max} = 358$ nm, $\epsilon_{max} = 1.8 \times 10^4$ M^{-1} cm^{-1}), $AcrPh^+$ ($\lambda_{max} = 360$ nm, $\epsilon_{max} = 1.8 \times 10^4$ M^{-1} cm^{-1}), and $AcrCH_2Ph^+$ ($\lambda_{max} = 360$ nm, $\epsilon_{max} = 1.8 \times 10^4$ M^{-1} cm^{-1}), respectively, where the DCA absorbance at 422 nm has been taken into account. To avoid the contribution of light absorption of the products, only the initial rates were determined for determination of the quantum yields.

$^1O_2$ Phosphorescence Measurements. An O_2-saturated CD_3CN solution containing DCA (2.5×10^{-4} M) in quartz cells (optical path length 10 mm) was excited at $\lambda = 422$ nm using a Cosmo System LVU-200S spectrometer. Nanosecond pulse for sample excitation ($\lambda = 422$ nm) was obtained by the dye laser (Usho Optical Systems DL50) with the coumarin 120 in methanol (0.12 g/L), where the dye was excited by the frequency tripled output ($\lambda = 355$ nm) of the *Q*-switched Nd:YAG laser (Spectra Physics GCR-150−10) operating at 10 Hz. Typical pulse energies at the sample were in the range of 1−2 mJ. A photomultiplier (Hamamatsu Photonics, R5509−72) cooled by liquid nitrogen was used to detect emission from the sample cell in the near-infrared region through the slit with 2 mm width and a monochromator equipped with diffraction gratings appropriate for the infrared light. The signal was captured and averaged by a digital storage oscilloscope (Tektronix TDS3032) and transferred to a personal computer for analysis. Typical decays were recorded as the average of 32 laser shots. The decays were analyzed with nonlinear least-squares analysis of the observed time profile with a single-exponential function and in all cases gave good quality fits.

The $^1O_2$ phosphorescence lifetimes were measured for CD_3CN solutions containing DCA (2.5×10^{-4} M) with $AcrH_2$ and $AcrD_2$ in the absence and presence of $Sc(OTf)_3$. There was no change in the shape of the phosphorescence spectra, but there was a change in the phosphorescence lifetime by the addition of a quencher. The Stern−Volmer relationship (eq 1) was obtained for the ratio of the phosphorescence lifetimes in

$$\tau_0/\tau = 1 + k_q\tau_0[D] \quad (1)$$

the absence and presence of $Sc(OTf)_3$ and the concentrations of $AcrH_2$ and $AcrD_2$ used as quenchers (τ_0 is the lifetime in the absence of a quencher).

Fluorescence Quenching. Quenching experiments of the fluorescence of DCA were carried out on a Shimadzu spectrofluorophotometer (RF-5000). The excitation wavelength of DCA was 422 nm in MeCN. The monitoring wavelength was corresponding to the maximum of the emission band at $\lambda_{max} = 435$ nm. Typically, an MeCN solution (3.0 cm^3) was deaerated by argon purging for 8 min prior to the measurements. Relative fluorescence intensities were measured for MeCN solutions containing DCA (1.0×10^{-5} M), electron donors and O_2. There was no change in the shape, but there was a change in the intensity of the fluorescence peak by the addition of a quencher. The Stern−Volmer relationship (eq 2) was obtained for the ratio of the emission intensities and the concentrations of electron

$$I_0/I = 1 + K_{SV}[D] \quad (2)$$

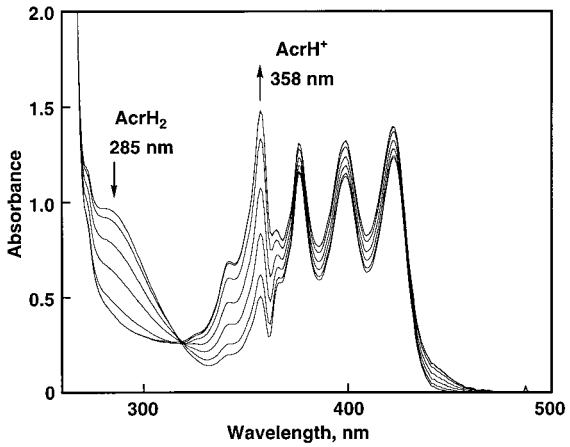

Figure 1. UV-visible spectral change in the photooxidation of $AcrH_2$ (5.0×10^{-5} M) in the presence of DCA (1.0×10^{-4} M) and Sc^{3+} (2.0×10^{-4} M) in O_2 saturated MeCN under irradiation of visible light ($\lambda > 380$ nm) at 298 K; interval 150 s.

donors and O_2 used as quenchers.[29] The observed quenching rate constants k_q ($=K_{SV}\tau^{-1}$) were obtained from the Stern−Volmer constants K_{SV} and the fluorescence lifetime τ (19.6 ns).[30]

ESR Measurements. The ESR spectra of the $O_2^{\bullet-}-Sc^{3+}$ complex were measured using a JEOL JES−FA 100 X-band spectrometer with a low-temperature cooling apparatus. An O_2-saturated propionitrile solution of $AcrH_2$ (3.6×10^{-5} M), DCA (2.5×10^{-4} M), and $Sc(OTf)_3$ (1.0×10^{-2} M) was irradiated at 193 K with a high-pressure mercury lamp (USH-1005D) through a cut off filter (Toshiba UV-37) transmitting $\lambda > 380$ nm focusing at the sample cell in the ESR cavity. The ESR spectra were recorded under nonsaturating microwave power conditions. The magnitude of modulation was chosen to optimize the resolution and signal-to-noise (S/N) ratio of the observed spectra. The *g* values and hyperfine splitting constants (hfs) were calibrated using an Mn^{2+} marker.

Laser Flash Photolysis. The measurements of transient absorption spectra in the photooxidation of $AcrH_2$ (2.8×10^{-4} M) in the presence of DCA (1.2×10^{-4} M) and $Sc(OTf)_3$ (0, 1.0×10^{-3} M) were performed according to the following procedures. The O_2 saturated MeCN solution containing DCA (1.2×10^{-4} M), $AcrH_2$ (2.8×10^{-4} M), and $Sc(OTf)_3$ (0, 1.0×10^{-3} M) was excited by a Nd:YAG laser (Quanta-Ray, GCR-130, 6 ns fwhm) at $\lambda = 425$ nm with the power of 10 mJ per pulse. A Xe flash lamp was used for the probe beam, which was detected with a Si-PIN module (Hamamatsu, S5343) after passing through the photochemical quartz vessel (10 mm × 10 mm) and a monochromator. The output from the Si-PIN module was recorded with a digitizing oscilloscope (HP 54510B, 300 MHz). The transient spectra were recorded using fresh solutions in each laser excitation. All experiments were performed at 298 K.

Results and Discussion

Sc^{3+}−Promoted DCA−Photosensitized Oxidation of AcrHR with Oxygen. When an O_2-saturated MeCN solution containing $AcrH_2$ (5.0×10^{-5} M), DCA (1.0×10^{-4} M), and $Sc(OTf)_3$ (2.0×10^{-4} M) is irradiated with the visible light ($\lambda > 380$ nm), the absorption band due to $AcrH^+$ ($\lambda_{max} = 358$ nm) appears and the absorbance increases with the concomitant disappearance of the absorption band due to $AcrH_2$ ($\lambda_{max} = 285$ nm), as shown in Figure 1. The quantitative formation of $AcrH^+$ has also been confirmed by the ^1H NMR (see the Experimental Section).[31] After the completion of the photochemical reaction, an approximately equivalent amount of hydrogen peroxide (95% based on the initial amount of $AcrH_2$) was formed (see the Experimental Section). Thus, the stoichiometry of the photochemical reaction is given by eq 3. Trifluoroacetic acid was added as a proton source (see the Experimental Section). The DCA absorbance remains unchanged during the photooxidation of $AcrH_2$. This indicates that DCA acts as an efficient and stable photocatalyst for the photooxidation of $AcrH_2$ in the presence of Sc^{3+}. In the absence of Sc^{3+}, however, no photooxidation of $AcrH_2$ was observed with or without O_2 ($\lambda > 380$ nm). Without DCA no photooxidation of $AcrH_2$ occurs even in the presence of Sc^{3+} under otherwise the same experimental conditions. Thus, both DCA and Sc^{3+} are required for the photooxidation of $AcrH_2$.

TABLE 1: Photooxidation of AcrHR (6.0×10^{-3} M) in the Presence of DCA (3.0×10^{-4} M), CF_3COOH (1.0×10^{-2} M), and Sc^{3+} (3.0×10^{-4} M) in O_2 Saturated CD_3CN under Irradiation of Visible Light ($\lambda > 380$ nm) for 1 h at 298 K

AcrHR	product (yield, %)	
$AcrH_2$	$AcrH^+$ (100)	H_2O_2 (95)
AcrHMe	$AcrHMe^+$ (100)	H_2O_2 (90)
AcrHEt	$AcrHEt^+$ (100)	H_2O_2 (97)
AcrHPh	$AcrPh^+$ (100)	H_2O_2 (87)
$AcrHCH_2Ph$	$AcrHCH_2Ph^+$ (75)	H_2O_2 (75)
	$AcrH^+$ (25)	PhCHO (10), $PhCH_2COOH$ (15)
$AcrHBu^t$	$AcrH^+$ (100)	Bu^tOOH (76), Bu^tOH (24)
$(AcrH)_2$	$AcrH^+$ (100)	H_2O_2 (86)

Other 9-substituted AcrHR can also be oxidized by the DCA photosensitization in the presence of Sc^{3+} in MeCN. As is the case of $AcrH_2$, AcrHR with R = Me, Et, and Ph is dehydrogenated to yield $AcrR^+$ accompanied by formation of H_2O_2. These product yields are listed in Table 1. In contrast to these dehydrogenation reactions, the DCA-sensitized photooxidation of AcrHR containing tertiary alkyl group (R = Bu^t) yields the oxygenated product of the *tert*-butyl group, i.e, Bu^tOOH and Bu^tOH, together with $AcrH^+$ (eq 4). In this case, the C(9)−C bond is cleaved to undergo the oxygenation reaction rather than the dehydrogenation via the C(9)−H bond cleavage. In the case of the dimer (R = AcrH), the C(9)−C bond is also cleaved selectively to yield $AcrH^+$ accompanied by formation of H_2O_2 (Table 1). In the case of a secondary alkyl group (R = CH_2-Ph), both the C(9)−H and C(9)−C bonds are cleaved to yield the two types of products shown in eqs 3 and 4 (Table 1).

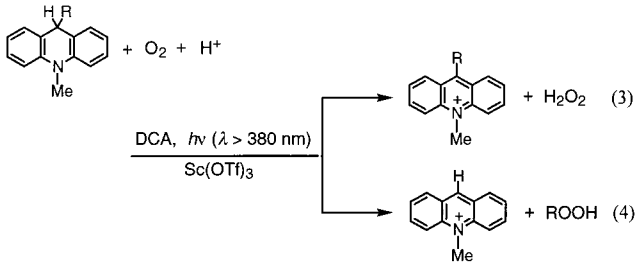

The observed selectivities for the C(9)−H vs C(9)−C bond cleavage in Table 1 agree with those reported for the cleavage of radical cations of AcrHR ($AcrHR^{\bullet+}$) depending on the type of substituent R.[20] Such an agreement indicates that the DCA-photosensitized oxidation of AcrHR occurs via $AcrHR^{\bullet+}$ which may be produced by electron transfer from AcrHR to the singlet excited state of DCA ($^1DCA^*$). Alternatively, $AcrHR^{\bullet+}$ may be produced via electron transfer from AcrHR to singlet oxygen ($^1O_2$), because singlet oxygen ($^1O_2$) is known to be produced efficiently via an energy transfer from $^1DCA^*$ to O_2.[14] Thus, the possibility of involvement of $^1O_2$ in the DCA-photosensitized

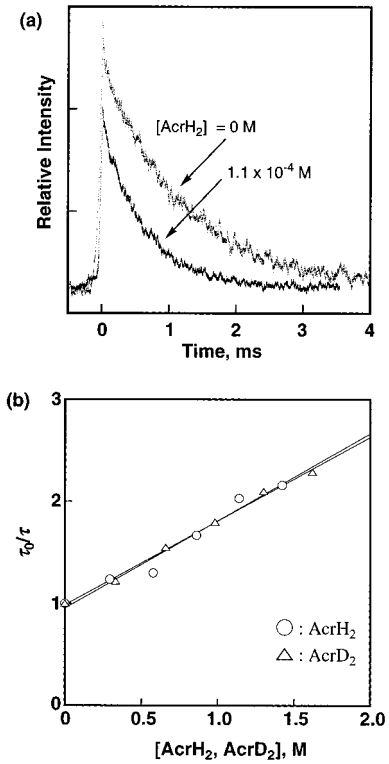

Figure 2. (a) Decay curves of phosphorescence of $^1O_2$ at $\lambda_{max} = 1270$ nm in the absence and presence of $AcrH_2$ after laser excitation ($\lambda = 422$ nm) in CD_3CN at 298 K. (b) Stern−Volmer plot for the phosphorescence quenching of $^1O_2$ by $AcrH_2$ in CD_3CN at 298 K.

oxidation of AcrHR in the presence of Sc^{3+} was examined in detail (vide infra).

Singlet Oxygen vs Electron Transfer. The $^1O_2$ phosphorescence at 1270 nm is observed upon laser excitation of an O_2-saturated CD_3CN solution containing DCA (2.5×10^{-4} M). The decay of $^1O_2$ phosphorescence obeys first-order kinetics, and the lifetime (1.0 ms) agreed with the literature data.[32,33] The addition of $AcrH_2$ as a quencher results in a decrease in the $^1O_2$ lifetime as shown in Figure 2a. The Stern−Volmer plot (eq 1) gives a good linear correlation between τ_0/τ and the quencher concentration (Figure 2b). The quenching rate constant (k_q) is determined as 7.0×10^7 M^{-1} s^{-1} from the slope of the linear plot. It was confirmed that the k_q value was independent of the Sc^{3+} concentration.

When $AcrH_2$ is replaced by the dideuterated compound ($AcrD_2$), eventually, the same k_q value is obtained as shown in Figure 2b (compare the open circle with triangle for $AcrH_2$ and $AcrD_2$, respectively). Thus, there is no kinetic isotope effect in the $^1O_2$ quenching by $AcrH_2$ and $AcrD_2$. The absence of the kinetic isotope effect indicates that no transfer of hydrogen is involved in the rate-determining step of the $^1O_2$ quenching by $AcrH_2$. This is consistent with a number of reported examples of the $^1O_2$ quenching via formation of exciplexes with electron donors in which only a partial charge transfer occurs.[34−38] The full electron transfer from $AcrH_2$ to $^1O_2$ is unlikely to occur judging from the more positive one-electron oxidation potential of $AcrH_2$ (E^0_{ox} vs SCE = 0.81 V)[20] than the one-electron reduction potential of $^1O_2$ in MeCN (E^{0*}_{red} vs SCE = 0.11 V).[39,40]

New absorption bands appear at 510, 640, and 710 nm after the laser excitation (425 nm) of the absorption band of DCA (1.2×10^{-4} M) in MeCN containing $AcrH_2$ (2.8×10^{-4} M) at 1.4 μs as shown in Figure 3. Because the absorption at 640 nm is significantly large as compared to other absorptions at 510

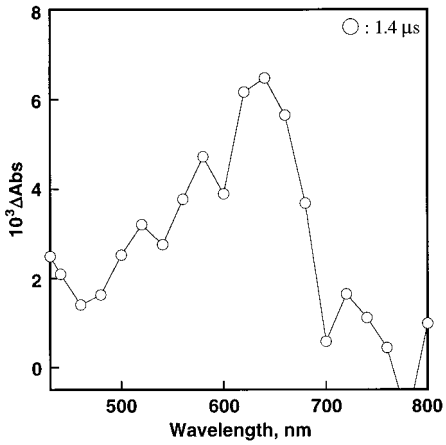

Figure 3. Transient absorption spectrum in the photooxidation of $AcrH_2$ (2.8×10^{-4} M) in the presence of DCA (1.2×10^{-4} M) in O_2 saturated MeCN at 298 K (laser excitation at $\lambda = 425$ nm).

and 710 nm of $DCA^{\bullet-}$,[41] an absorption due to $AcrH_2^{\bullet+}$ ($\lambda_{max} = 640$ nm)[20] may be overlapped with the absorption due to $DCA^{\bullet-}$ in Figure 3. The formation of $AcrH_2^{\bullet+}$ is completed within 1 μs, and no further rise of the absorption due to $AcrH_2^{\bullet+}$ is observed.

The rate constant of electron transfer from $AcrH_2$ to $^1DCA^*$ is determined by the fluorescence quenching (see the Experimental Section) as 2.8×10^{10} M^{-1} s^{-1} which is a diffusion-limited value. Such a fast electron transfer is consistent with the highly exergonic nature of the reaction: the free energy change of electron transfer (ΔG^0_{et}) is determined as −1.10 eV from the E^0_{ox} value of $AcrH_2$ (0.81 V)[20] and the E^0_{red} value of $^1DCA^*$ (1.91 V).[30] On the other hand, the DCA fluorescence ($\tau_0 = 19.6$ ns)[30] is also quenched by oxygen via an energy transfer with the rate constant of 3.2×10^9 M^{-1} s^{-1} (see the Experimental Section).[42] Thus, an energy transfer and electron transfer are competing and the relative ratio depends on the concentration ratio of $AcrH_2$ and O_2. In any case, the formation of $AcrH_2^{\bullet+}$ via photoinduced electron transfer from $AcrH_2$ to $^1DCA^*$ would be prompt and readily distinguishable from the microsecond or millisecond time scale for the reaction of $AcrH_2$ with $^1O_2$ (Figure 2). Thus, it can be concluded that $AcrH_2^{\bullet+}$ is formed via photoinduced electron transfer from $AcrH_2$ to $^1DCA^*$ and not from $AcrH_2$ to $^1O_2$.

The quantum yields (Φ) for the formation of $AcrH^+$ in the DCA-photosensitized oxidation of $AcrH_2$ by O_2 in the presence of $Sc(OTf)_3$ in O_2-saturated MeCN are determined by varying the $AcrH_2$ and $Sc(OTf)_3$ concentrations (see the Experimental Section). The Φ value at a fixed concentration is independent of the $Sc(OTf)_3$ concentration as shown in Figure 4, although there is no photooxidation of $AcrH_2$ without $Sc(OTf)_3$ (vide supra). Thus, a small concentration of $Sc(OTf)_3$ (1.0×10^{-4} M) is enough to make it possible to undergo the DCA-photosensitized oxidation of $AcrH_2$ with O_2.[43] The effects of other metal ions on the Φ value are also examined using $Mg(ClO_4)_2$ and $Lu(OTf)_3$ (Figure 4). The $Sc(OTf)_3$ gives the higher Φ values as compared to the weaker Lewis acids, i.e., $Mg(ClO_4)_2$ and $Lu(OTf)_3$. The Φ value for the formation of $AcrH^+$ is proportional to the concentration of $AcrH_2$ at low concentrations (ca. 10^{-4} M) as shown in Figure 5. This is also consistent with the electron-transfer mechanism since the quenching efficiency of $^1DCA^*$ in the presence of 1×10^{-4} M $AcrH_2$ is 3% and increases linearly with increasing [$AcrH_2$]. In contrast to the case of the $^1O_2$ quenching by $AcrH_2$, an appreciable kinetic isotope effect ($\Phi_H/\Phi_D = 1.9$) is observed for the Φ value when $AcrH_2$ is replaced by $AcrD_2$ (open triangle in Figure 5).

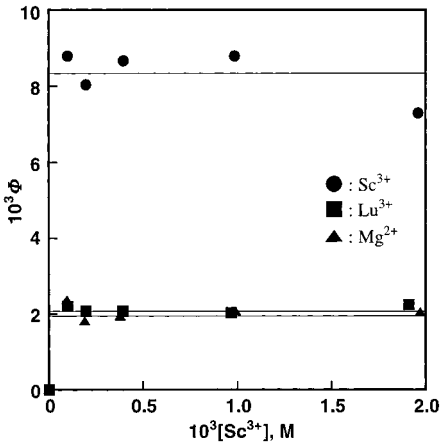

Figure 4. Dependence of the quantum yield (Φ) on $[M^{n+}]$ (M^{n+} = Sc^{3+} (●), Lu^{3+} (■), Mg^{2+} (▲)) for the photooxidation of $AcrH_2$ (1.8×10^{-4} M) in MeCN at 298 K.

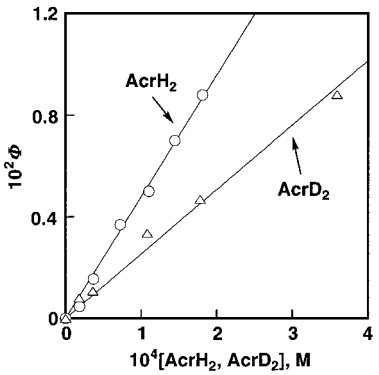

Figure 5. Dependence of the quantum yield (Φ) for the formation of $AcrH^+$ on $[AcrH_2, AcrD_2]$ ($AcrH_2$ (○), $AcrD_2$ (△)) for the DCA-photosensitized oxidation of $AcrH_2$ and $AcrD_2$ in the presence of Sc^{3+} (1.0×10^{-3} M) in MeCN at 298 K.

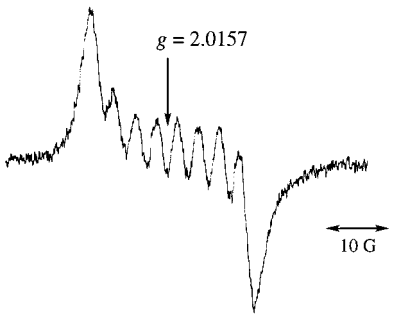

Figure 6. ESR spectrum of O_2 radical anion−Sc^{3+} complex produced in photooxidation of $AcrH_2$ (3.6×10^{-5} M) in the presence of DCA (2.5×10^{-4} M) and Sc^{3+} (1.0×10^{-2} M) in O_2 saturated EtCN at 193 K.

The observed kinetic isotope effect may be ascribed to a hydrogen transfer step from $AcrH_2^{\bullet+}$ to $O_2^{\bullet-}-Sc^{3+}$ produced via an electron transfer from $DCA^{\bullet-}$ to O_2 in the presence of Sc^{3+} as shown in Scheme 1. The singlet excited state (^{1}DCA*) is quenched by $AcrH_2$ and O_2 by an electron transfer and energy transfer to produce $AcrH_2^{\bullet+}$ and $^1O_2$, respectively. The $^1O_2$ is quenched by $AcrH_2$ via an exciplex formation which decays to the ground state. The radical ion pair produced by photoinduced electron transfer decays to the reactant pair via the back electron transfer from $DCA^{\bullet-}$ to $AcrH_2^{\bullet+}$. In competition with the back electron transfer, $DCA^{\bullet-}$ in the radical ion pair is oxidized by O_2 to produce ($AcrH_2^{\bullet+}$ $O_2^{\bullet-}-Sc^{3+}$) which also undergoes back electron transfer from $O_2^{\bullet-}-Sc^{3+}$ to $AcrH_2^{\bullet+}$ to the ground state.

SCHEME 1

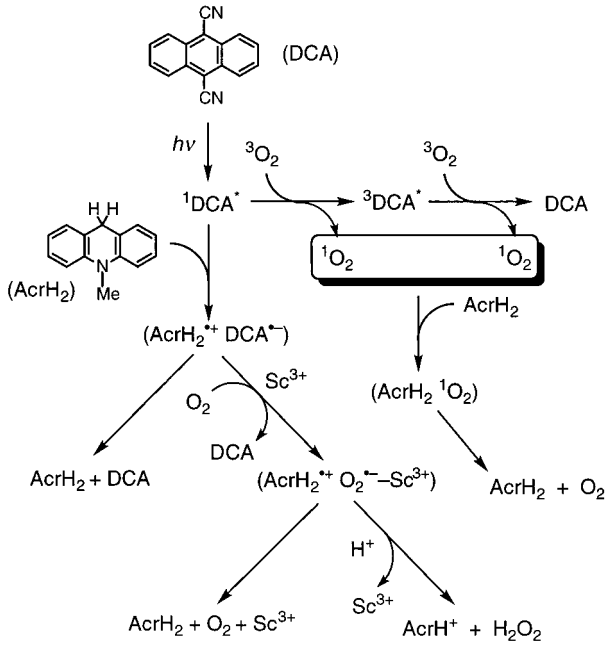

In competition with the back electron transfer, a hydrogen transfer from $AcrH_2^{\bullet+}$ to $O_2^{\bullet-}-Sc^{3+}$ occurs to yield the final product, $AcrH^+$ and H_2O_2 (after the protonation in Scheme 1).[44] In the absence of Sc^{3+}, $O_2^{\bullet-}$ is produced instead of $O_2^{\bullet-}-Sc^{3+}$ in Scheme 1, and the back electron transfer from $O_2^{\bullet-}$ to $AcrH_2^{\bullet+}$ may be much faster than a hydrogen transfer from $AcrH_2^{\bullet+}$ to $O_2^{\bullet-}$, because the back electron transfer is highly exergonic ($\Delta G^0_{et} = -1.68$ eV),[45] and the reactivity of $O_2^{\bullet-}$ is much smaller than $O_2^{\bullet-}-Sc^{3+}$ in which the unpaired electron is more localized on the terminal oxygen atom.[22] In the presence of Sc^{3+}, $O_2^{\bullet-}$ is known to form the complex $O_2^{\bullet-}-Sc^{3+}$.[22] Because of the strong binding of Sc^{3+} to $O_2^{\bullet-}$, $O_2^{\bullet-}-Sc^{3+}$ is harder to oxidize than $O_2^{\bullet-}$, thus retarding the back electron transfer to $AcrH_2^{\bullet+}$.[46,47]

The formation of $O_2^{\bullet-}-Sc^{3+}$ as a reactive intermediate for the DCA-photosensitized oxidation of $AcrH_2$ is confirmed by the ESR measurements of an O_2-saturated propionitrile solution containing $AcrH_2$ (3.6×10^{-5} M), DCA (2.5×10^{-4} M), and $Sc(OTf)_3$ (1.0×10^{-2} M) at 193 K under photoirradiation with a Xe lamp ($\lambda > 380$ nm).[48] Figure 6 shows the observed ESR spectrum under the photoirradiation. The clear eight-line isotropic spectrum at the center is ascribed to the superhyperfine coupling of $O_2^{\bullet-}$ with the $^7/_2$ nuclear spin of the scandium nucleus ($a_{Sc} = 4.21$ G) in $O_2^{\bullet-}-Sc^{3+}$ as reported previously.[39] The isotropic g value (2.0157) is appreciably smaller than the corresponding value (2.030) of uncomplexed $O_2^{\bullet-}$ at 77 K, being consistent with the spin delocalization to the scandium nucleus as demonstrated by observation of superhyperfine.[22]

The quantum yields of DCA-photosensitized oxidation of other substituted compounds (AcrHR) also exhibit linear dependence on [AcrHR] as shown in Figure 7. The quantum yield increases in order: R = Ph < Et < Me < H < CH_2Ph < Bu^t < AcrH. This order agrees with the reactivity order of $AcrHR^{\bullet+}$,[20] supporting the electron-transfer mechanism in Scheme 1. In the case of $AcrHBu^t$, photoinduced electron transfer from $AcrHBu^t$ to ^{1}DCA* in the presence of O_2 and Sc^{3+} leads to formation of the radical ion pair ($AcrHBu^{t\bullet+}$ $O_2^{\bullet-}-Sc^{3+}$) as in the case of $AcrH_2$ (Scheme 1). The Bu^t group of $AcrHBu^{t\bullet+}$ is transferred to $O_2^{\bullet-}-Sc^{3+}$ via cleavage of the C(9)−C bond in competition with the back electron transfer

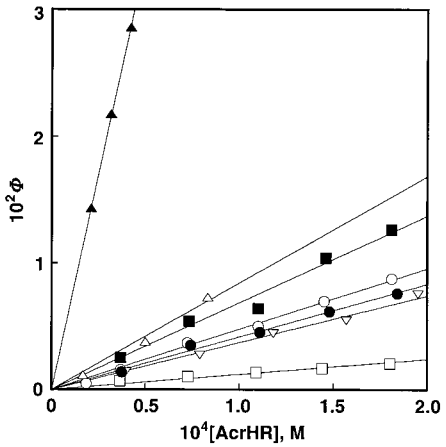

Figure 7. Dependence of the quantum yield (Φ) on [AcrHR] (R = H (○), Bu^t (△), Et (▽), Ph (□), Me (●), CH_2Ph (■), AcrH (▲)) for the photooxidation of AcrHR in the presence of DCA (1.0×10^{-4} M) and Sc^{3+} (1.0×10^{-3} M) in O_2 saturated MeCN at 298 K.

SCHEME 2

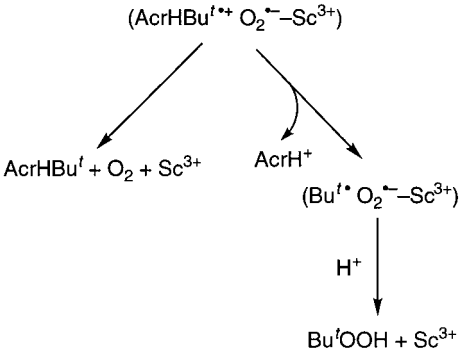

from $O_2^{\bullet-}-Sc^{3+}$ to AcrHBu$^{t\bullet+}$ to yield Bu^{t}OOH (Scheme 2). The Bu^{t}OOH decomposes further to Bu^{t}OH (Table 1). The C(9)−C bond is also cleaved in $(AcrH)_2^{\bullet+}$, resulting in formation of AcrH$^\bullet$ which can further reduce $O_2^{\bullet-}-Sc^{3+}$ to yield $AcrH^+$ and H_2O_2.

Electron-Transfer Radical Chain Mechanism. According to Scheme 1, the quantum yield would reach the limiting value which is determined by the competition between the hydrogen transfer from $AcrH_2^{\bullet+}$ to $O_2^{\bullet-}-Sc^{3+}$ and the back electron transfer. However, the quantum yield increases linearly with a further increase in the $AcrH_2$ concentration, exceeding unity as shown in Figure 8a.[49] The kinetic isotope effect Φ_H/Φ_D is also determined using $AcrD_2$ as 3.0 (Figure 8a), which is different from the value (1.9) determined at the low concentration range (Figure 5). Such a difference in the kinetic isotope effects suggests the change in the reaction mechanism depending on the $AcrH_2$ concentration. The dependence of the Φ value on the light intensity at fixed $AcrH_2$ concentrations is also examined as shown in Figure 8b, where the Φ value is proportional to reciprocal of the square root of light intensity. The large quantum yields exceeding unity, combined with the dependence of Φ on the $AcrH_2$ concentration (Figure 8a) and on the light intensity (Figure 8b), indicate strong involvement of radical chain processes which are initiated by the photoinduced electron-transfer reactions as shown in Scheme 3.

The $AcrH_2^{\bullet+}$ in the radical ion pair ($AcrH_2^{\bullet+}$ $O_2^{\bullet-}-Sc^{3+}$) in Scheme 1 may escape from the cage to give the deprotonated radical (AcrH$^\bullet$) which can start the radical chain propagation in Scheme 3. First, an electron transfer from AcrH$^\bullet$ to O_2 occurs efficiently in the presence of Sc^{3+} to give $O_2^{\bullet-}-Sc^{3+}$ which is converted to $HO_2^\bullet$.[21,50] In the propagation step, $HO_2^\bullet$ abstracts

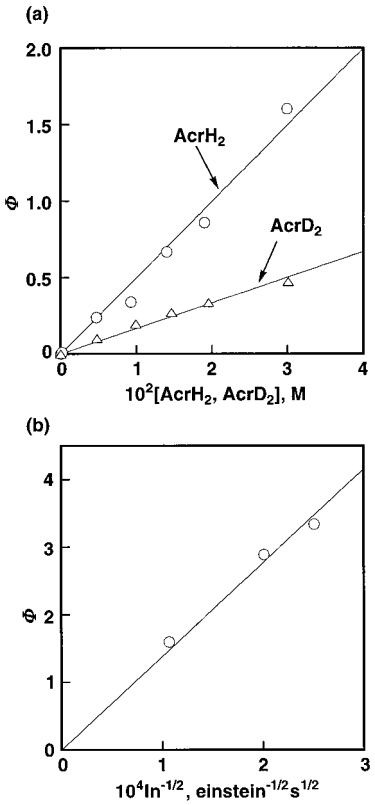

Figure 8. (a) Dependence of the quantum yield (Φ) on [$AcrH_2$, $AcrD_2$] ($AcrH_2$ (○), $AcrD_2$ (△)) for the DCA-photosensitized oxidation of $AcrH_2$ and $AcrD_2$ in the presence of DCA (1.0×10^{-4} M) and Sc^{3+} (1.0×10^{-3} M) in O_2 saturated MeCN at 298 K; the irradiation light intensity: 1.6×10^{-9} einstein s^{-1}. (b) Dependence of the quantum yield (Φ) on light intensity (*In*) for the DCA-photosensitized oxidation of $AcrH_2$ (3.0×10^{-2} M) in the presence of DCA (1.0×10^{-4} M) and Sc^{3+} (1.0×10^{-3} M) in O_2 saturated MeCN at 298 K.

SCHEME 3

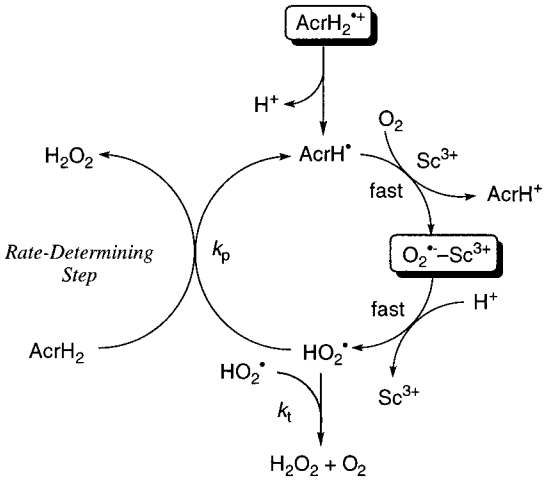

a hydrogen from $AcrH_2$ to yield H_2O_2, accompanied by regeneration of AcrH$^\bullet$ (Scheme 3). Such electron-transfer radical chain reactions are also started by $O_2^{\bullet-}-Sc^{3+}$ escaped from the radical ion pair ($AcrH_2^{\bullet+}$ $O_2^{\bullet-}-Sc^{3+}$). The rate-determining step may be the hydrogen transfer from $AcrH_2$ to $HO_2^\bullet$ because the observed kinetic isotope effect (3.0) agrees with that reported for the hydrogen abstraction reaction of $HO_2^\bullet$ from $AcrH_2$.[7] This may be the reason the kinetic isotope effect is changed from the low $AcrH_2$ concentration range (Figure 5) where the contribution of the radical chain reactions is negligible and the

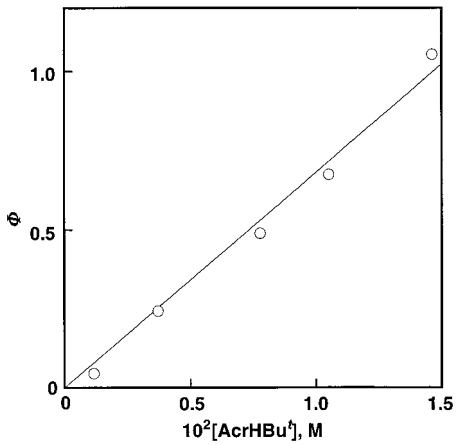

Figure 9. Dependence of the quantum yield (Φ) on [AcrHBu^t] for the photooxidation of AcrHBu^t in the presence of DCA (1.0×10^{-4} M) and Sc^{3+} (1.0×10^{-3} M) in O_2 saturated MeCN at 298 K.

SCHEME 4

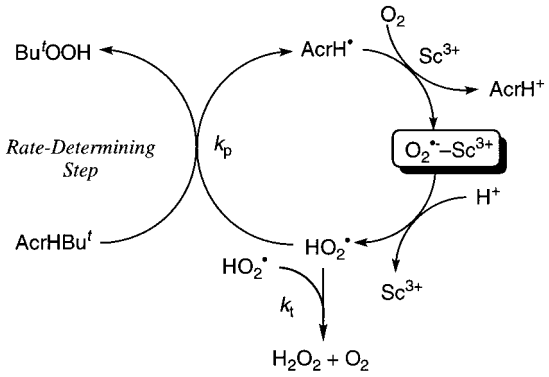

Φ_H/Φ_D value is ascribed to the hydrogen transfer from $AcrH_2^{\bullet+}$ to $O_2^{\bullet-}-Sc^{3+}$ (Scheme 1).

By applying the steady-state approximation to the radical species ($HO_2^\bullet$ and AcrH$^\bullet$) in Scheme 1, the quantum yield (Φ) is given as the function of the light intensity (*In*) and the concentration of $AcrH_2$ (eq 5)

$$\Phi = k_p(\Phi_0/k_t In)^{1/2}[AcrH_2] \qquad (5)$$

where Φ_0 is the quantum yield of the initiation step, k_p is the rate constant of the rate-determining propagation step, and k_t is the rate constant of the termination step (see the Supporting Information S1 for the derivation of eq 5). The derived dependence of Φ on [$AcrH_2$] agrees with the experimental results that the Φ value is proportional to the $AcrH_2$ concentration (Figure 8a) and the reciprocal of the square root of the light intensity (Figure 8b) and independent of the Sc^{3+} concentration (Figure 4).

In the case of AcrHBu^t as well, the Φ value increases linearly with a further increase in the AcrHBu^t concentration, exceeding unity (Figure 9). Eventually the same radical chain mechanism as Scheme 3 may be applied to the DCA-photosensitized oxygenation of AcrHBu^t. In the propagation step, however, the C(9)−C bond of AcrHBu^t is cleaved rather than the C(9)−H bond to yield Bu^{t}OOH as shown in Scheme 4.

Conclusions

In summary, photooxidation of AcrHR with O_2 occurs efficiently in the presence of DCA and Sc^{3+} under visible light irradiation in O_2-saturated MeCN to yield $AcrR^+$ and H_2O_2 or $AcrH^+$ and the oxygenated products of R such as ROOH, depending on the type of substituent R. The observed selectivities for the C(9)−H vs C(9)−C bond cleavage of AcrHR in the DCA-photosensitized oxidation of AcrHR in the presence of Sc^{3+} result from those for the cleavage of the C(9)−H vs C(9)−C bond of $AcrHR^{\bullet+}$ depending on the type of substituent R. The photoinduced electron transfer from AcrHR to ^{1}DCA* starts the electron-transfer radical chain reactions (Schemes 3 and 4) to yield the oxidation products. The essential role of Sc^{3+} for the DCA-photosensitized oxidation of AcrHR may be the strong binding of Sc^{3+} to $O_2^{\bullet-}$, which retards the back electron transfer leading to the oxidation of AcrHR. Singlet oxygen plays no essential role in the oxidation of AcrHR.

Acknowledgment. This work was partially supported by a Grant-in-Aid for Scientific Research Priority Area (No. 11228205) from the Ministry of Education, Science, Culture and Sports, Japan.

Supporting Information Available: Derivation of eq 5 (S1). This material is available free of charge via the Internet at http://pubs.acs.org.

References and Notes

(1) Stryer, L. *Biochemistry*; Freeman: New York, 1988; Chapter 17.
(2) Babcock, G. T.; Wikström, M. *Nature (London)* **1992**, *356*, 301.
(3) (a) Fukuzumi, S. In *Photoinduced Electron Transfer*; Fox, M. A., Chanon, M., Eds.; Elsevier: Amsterdam, 1988; Part C, Chapter 10. (b) Chanon, M.; Julliard, M.; Santamaria, J.; Chanon, F. *New J. Chem.* **1992**, *16*, 171.
(4) (a) Bodaness, R. S.; Chan, P. C. *J. Biol. Chem.* **1977**, *252*, 8554. (b) Land, R. J.; Swallow, A. J. *Biochim. Biophys. Acta* **1971**, *234*, 34.
(5) Czochralska, B.; Kawczynski, W.; Bartosz, G.; Shugar, D. *Biochim. Biophys. Acta* **1984**, *801*, 403.
(6) Cunningham, M. L.; Johnson, J. S.; Giovanazzi, S. M.; Peak, M. J. *Photochem. Photobiol.* **1985**, *42*, 125.
(7) Fukuzumi, S.; Ishikawa, M.; Tanaka, T. *J. Chem. Soc., Perkin Trans. 2* **1989**, 1037.
(8) (a) Foote, C. S. *Acc. Chem. Res*. **1968**, *1*, 104. (b) Kearns, D. R. *Chem. Rev.* **1971**, *71*, 395. (c) Stephenson, L. M.; Grdina, M. J.; Orfanopoulos, M. *Acc. Chem. Res.* **1980**, *13*, 419. (d) Foote, C. S.; Clennan, E. L. *Properties and Reactions of Singlet Oxygen. In Active Oxygen in Chemistry*; Foote, C. S., Valentine, J. S., Greenberg, A., Liebman, J. F., Eds.; Chapman and Hall: New York, 1995; pp 105−140.
(9) (a) Bellus, D. *Adv. Photochem*. **1979**, *11*, 105. (b) Gorman, A. A. *Adv. Photochem*. **1992**, *17*, 217. (c) Lissi, E. A.; Encinas, M. V.; Lemp, E.; Rubio, M. A. *Chem. Rev*. **1993**, *93*, 699. (d) Adam, W.; Prein, M. *Acc. Chem. Res*. **1996**, *29*, 275.
(10) (a) Sheu, C.; Foote, C. S. *J. Am. Chem. Soc*. **1995**, *117*, 474. (b) Sheu, C.; Foote, C. S. *J. Am. Chem. Soc*. **1995**, *117*, 6439. (c) Adam, W.; Saha-Möller, C. R.; Schönberger, A. *J. Am. Chem. Soc*. **1996**, *118*, 9233. (d) Raoul, S.; Cadet, J. *J. Am. Chem. Soc*. **1996**, *118*, 1892.
(11) (a) Duarte, V.; Gasparutto, D.; Yamaguchi, L. F.; Ravanat, J.-L.; Martinez, G. R.; Medeiros, M. H. G.; Mascio, P. D.; Cadet, J. *J. Am. Chem. Soc.* **2000**, *122*, 12622. (b) Greer, A.; Vassilikogiannakis, G.; Lee, K.-C.; Koffas, T. S.; Nahm, K.; Foote, C. S. *J. Org. Chem.* **2000**, *65*, 6876. (c) Bobrowski, M.; Liwo, A.; Oldziej, S.; Jeziorek, D.; Ossowski, T. *J. Am. Chem. Soc.* **2000**, *122*, 8112. (d) Adam, W.; Peters, K.; Peters, E.-M.; Schambony, S. B. *J. Am. Chem. Soc.* **2000**, *122*, 7610. (e) Cermola, F.; Lorenzo, F. D.; Giordano, F.; Graziano, M. L.; Iesce, M. R.; Palumbo, G. *Org. Lett.* **2000**, *2*, 1205. (f) Abdel-Shafi, A. A.; Wilkinson, F. *J. Phys. Chem. A* **2000**, *104*, 5747. (g) Bernstein, R.; Foote, C. S. *J. Phys. Chem. A* **1999**, *103*, 7244.
(12) (a) Yoshioka, M.; Sakuma, Y.; Saito, M. *J. Org. Chem.* **1999**, *64*, 9247. (b) Dussault, P. H.; Schultz, J. A. *J. Org. Chem.* **1999**, *64*, 8419. (c) Toutchkine, A.; Clennan, E. L. *J. Org. Chem.* **1999**, *64*, 5620. (d) Mori, H.; Ikoma, K.; Isoe, S.; Kitaura, K.; Katsumura, S. *J. Org. Chem.* **1998**, *63*, 8704. (e) Stratakis, M.; Orfanopoulos, M.; Foote, C. S. *J. Org. Chem.* **1998**, *63*, 1315. (f) Nojima, T.; Ishiguro, K.; Sawaki, Y. *J. Org. Chem.* **1997**, *62*, 6911. (g) Ishiguro, K.; Hayashi, M.; Sawaki, Y. *J. Am. Chem. Soc.* **1996**, *118*, 7265. (h) Fukuzumi, S.; Tanii, K.; Tanaka, T. *J. Chem. Soc., Perkin Trans. 2* **1989**, 2103.
(13) Araki, Y.; Dobrowolski, D. C.; Goyne, T. E.; Hanson, D. C.; Jiang, Z. Q.; Lee, K. J.; Foote, C. S. *J. Am. Chem. Soc.* **1984**, *106*, 4570.
(14) (a) Kanner, R. C.; Foote, C. S. *J. Am. Chem. Soc*. **1992**, *114*, 678. (b) Kanner, R. C.; Foote, C. S. *J. Am. Chem. Soc.* **1992**, *114*, 682. (c)

Manring, L. E.; Foote, C. S. *J. Phys. Chem.* **1982**, *86*, 1257. (d) Spada, L. T.; Foote, C. S. *J. Am. Chem. Soc*. **1980**, *102*, 391. (e) Marning, L. E.; Gu, C.-L.; Foote, C. S. *J. Phys. Chem*. **1983**, *87*, 40. (f) Dobrowolski, D. C.; Ogilby, P. R.; Foote, C. S. *J. Phys. Chem.* **1983**, *87*, 2261.

(15) (a) Cao, Y.; Zhang, B. W.; Ming, Y. F.; Chen, J. X. *J. Photochem.* **1987**, *38*, 131. (b) Santamaria, J. *Tetrahedron Lett.* **1981**, *22*, 4511. (c) Steichen, D. S.; Foote, C. S. *Tetrahedron Lett.* **1979**, 4363.

(16) Foote, C. S. *Tetrahedron* **1985**, *41*, 2221.

(17) Gollnick, K.; Schnatterer, A. *Photochem. Photobiol.* **1986**, *43*, 365.

(18) Lewis, F. D. In *Photoinduced Electron Transfer*; Fox, M. A., Chanon, M., Ed.; Elsevier: Amsterdam, 1988; Part C, Chapter 4.

(19) Hickerson, R. P.; Prat, F.; Muller, J. G.; Foote, C. S.; Burrows, C. J. *J. Am. Chem. Soc.* **1999**, *121*, 9423.

(20) Fukuzumi, S.; Tokuda, Y.; Kitano, T.; Okamoto, T.; Otera, J. *J. Am. Chem. Soc*. **1993**, *115*, 8960.

(21) Fukuzumi, S.; Patz, M.; Suenobu, T.; Kuwahara, Y.; Itoh, S. *J. Am. Chem. Soc*. **1999**, *121*, 1605.

(22) Fukuzumi, S.; Ohkubo, K. *Chem. Eur. J*. **2000**, *6*, 4532.

(23) Roberts, R. M. G.; Ostović, D.; Kreevoy, M. M. *Faraday Discuss. Chem. Soc.* **1982**, *74*, 257.

(24) Fukuzumi, S.; Koumitsu, S.; Hironaka, K.; Tanaka, T. *J. Am. Chem. Soc*. **1987**, *109*, 305

(25) Fukuzumi, S.; Kitano, T.; Mochida, K. *J. Am. Chem. Soc.* **1990**, *112*, 3246.

(26) Hatchard, C. G.; Parker, C. A. *Proc. R. Soc. London, Ser.* A **1956**, *235*, 518.

(27) Perrin, D. D.; Armarego, W. L. F.; Perrin, D. R. *Purification of Laboratory Chemicals*; Pergamon Press: Elmsford, NY, 1988.

(28) Fukuzumi, S.; Kuroda, S.; Tanaka, T. *J. Am. Chem. Soc.* **1985**, *107*, 3020.

(29) The different O_2 concentration in MeCN was obtained by changing the flow rate of O_2 and N_2 bubbled in an MeCN solution. The O_2 concentrations in MeCN were determined by the spectroscopic titration for the direct photooxidation of $AcrH_2$ by O_2 under UV-light irradiation; see: Fukuzumi, S.; Ishikawa, M.; Tanaka, T. *J. Chem. Soc., Perkin Trans. 2* **1989**, 1037.

(30) Eriksen, J.; Foote, C. S. *J. Phys. Chem*. **1978**, *82*, 2659.

(31) The small concentration of Sc^{3+} (3.0×10^{-4} M) is enough for the DCA-photosensitized photooxidation of $AcrH_2$ with O_2 (for the dependence of the quantum yield on the Sc^{3+} concentration, see Figure 4).

(32) (a) Wilkinson, F.; McGarvey, D. J.; Olea, A. F. *J. Am. Chem. Soc*. **1993**, *115*, 12144. (b) Wilkinson, F.; McGarvey, D. J.; Olea, A. F. *J. Phys. Chem*. **1994**, *98*, 3762. (c) Wilkinson, F.; Helman, W. P.; Ross, A. B. *J. Phys. Chem. Ref. Data* **1995**, *24*, 663. (d) Wilkinson, F.; Abdel-Shafi, A. A. *J. Phys. Chem. A* **1997**, *101*, 5509.

(33) A longer lifetime around 1.5 ms has been reported previously. See: Clough, R. L.; Dillon, M. P.; Iu, K.-K.; Ogilby, P. R. *Macromolecules* **1989**, *22*, 3620. This may indicate the presence of some $^1O_2$ quenching in the present system.

(34) (a) Darmanyan, A. P.; Jenks, W. S.; Jardon, P. *J. Phys. Chem. A* **1998**, *102*, 7420. (b) Darmanyan, A. P.; Jenks, W. S.; Jardon, P. *J. Phys. Chem. A* **1998**, *102*, 9308.

(35) (a) Darmanyan, A. P. *J. Phys. Chem. A* **1998**, *102*, 9833. (b) Darmanyan, A. P.; Lee, W.; Jenks, W. S. *J. Phys. Chem. A* **1999**, *103*, 2705.

(36) (a) Grewer, C.; Brauer, H.-D. *J. Phys. Chem*. **1994**, *98*, 4230. (b) Sato, C.; Kikuchi, K.; Okamura, K.; Takahashi, Y.; Miyashi, T. *J. Phys. Chem*. **1995**, *99*, 16925. (c) Nau, W. M.; Adam, W.; Scaiano, J. C. *J. Am. Chem. Soc*. **1996**, *118*, 2742. (d) Nau, W. M.; Scaiano, J. C. *J. Phys. Chem*. **1996**, *100*, 11360.

(37) (a) Schmidt, R.; Tanielian, C. *J. Phys. Chem. A* **2000**, *104*, 3177. (b) Li, C.; Hoffman, M. Z. *J. Phys. Chem. A* **2000**, *104*, 5998. (c) Schmidt, R.; Bodesheim, M. *J. Phys. Chem. A* **1998**, *102*, 4769.

(38) Clennan, E. L.; Wang, D.; Clifton, C.; Chen, M.-F. *J. Am. Chem. Soc*. **1997**, *119*, 9081.

(39) The E^0_{red} value is obtained by adding the excitation energy of $^1O_2$ (0.98 eV) to the E^0_{red} value of $^3O_2$ in the same solvent (−0.87 V).[40]

(40) Sawyer, D. T.; Chiericato, G., Jr.; Angelis, C. T.; Nanni, E. J., Jr.; Tsuchiya, T. *Anal. Chem.* **1982**, *54*, 1720.

(41) Fujita, M.; Ishida, A.; Majima, T.; Takamuku, S. *J. Phys. Chem.* **1996**, *100*, 5382.

(42) This value is consistent with the reported values (4.4×10^9 and 6.4×10^9 M^{-1} s^{-1}). See: (a) Olea, A. F.; Wilkinson, F. *J. Phys. Chem.* **1995**, *99*, 4518. (b) Kristiansen, M.; Scurlock, R. D.; Iu, K.-K.; Ogilby, P. R. *J. Phys. Chem.* **1991**, *95*, 5190.

(43) It was confirmed that the UV−visible spectral change at $[Sc^{3+}] = 2.0 \times 10^{-4}$ M (Figure 1) was virtually the same as the change at higher concentrations.

(44) The proton source here is H_2O ($\sim 10^{-2}$ M) contained in MeCN. The presence of additional proton source such as CF_3COOH (Table 1) does not affect the stoichiometry of the photochemical reaction (eqs 3 and 4).

(45) The ΔG^0_{et} value is obtained from the difference between the E^0_{ox} value of $AcrH_2$ (0.81 V)[22] and the E^0_{red} value of O_2 (−0.87 V).[40]

(46) Because the reorganization energy of the electron transfer of O_2 is know to be large (1.97 eV),[47] the back electron transfer may be in the Marcus normal region, when the rate of back electron transfer decreases with the decreasing the driving force of electron transfer.

(47) Lind, J.; Shen, X.; Merényi, G.; Jonsson, B. Ö. *J. Am. Chem. Soc*. **1989**, *111*, 7654.

(48) The slopes in Figure 8a are larger than the corresponding apparent slopes in Figure 5 because of the contribution of the nonchain process at low $AcrH_2$ or $AcrD_2$ concentrations. However, the degree of the contribution of the nonchain process is not determined quantitatively in this study. At high $AcrH_2$ or $AcrD_2$ concentrations in Figure 8a, the chain process certainly dominates as compared to the nonchain process.

(49) For the measurement of ESR, a high concentration of Sc^{3+} (1.0×10^{-2} M) is required to obtain the clear signal due to the $O_2^{\bullet -}-Sc^{3+}$ complex (Figure 6).

(50) The electron transfer from $AcrH^\bullet$ to O_2 is endothermic in MeCN, because the oxidation potential of $AcrH^\bullet$ (−0.43 V)[24] is more positive than the reduction potential of O_2 (−0.87 V).[40] In the presence of Sc^{3+}; however, the reduction potential of O_2 may be shifted in the positive direction,[22] making it possible that $AcrH^\bullet$ transfers an electron to O_2 to yield $AcrH^+$.